ACCOUNTS
of chemical research

Ultrafast Soft X-ray Photoelectron Spectroscopy at Liquid Water Microjets

M. FAUBEL,[†] K. R. SIEFERMANN,[‡] Y. LIU,[§] AND B. ABEL*[,§]

[†]*Max-Planck-Institut für Dynamik und Selbstorganisation, Bunsenstrasse 10, D-37073 Göttingen, Germany,* [‡]*Lawrence Berkeley National Laboratory, 1 Cyclotron Road 2-306, Berkeley, California 94720, United States , and* [§]*Wilhelm-Ostwald-Institute for Physical and Theoretical Chemistry, University Leipzig, Linnéstrasse 2, D-04103 Leipzig, Germany*

RECEIVED ON JUNE 8, 2011

CONSPECTUS

Since the pioneering work of Kai Siegbahn, electron spectroscopy for chemical analysis (ESCA) has been developed into an indispensable analytical technique for surface science. The value of this powerful method of photoelectron spectroscopy (PES, also termed photoemission spectroscopy) and Siegbahn's contributions were recognized in the 1981 Nobel Prize in Physics.

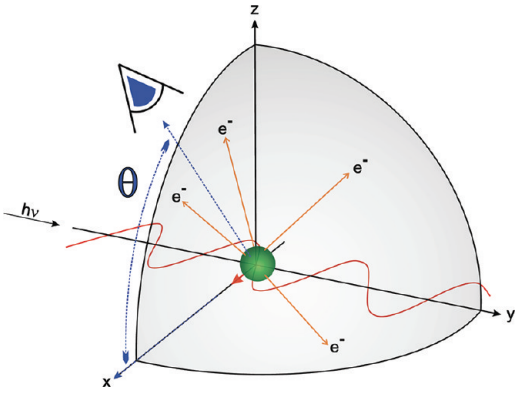

The need for high vacuum, however, originally prohibited PES of volatile liquids, and only allowed for investigation of low-vapor-pressure molecules attached to a surface (or close to a surface) or liquid films of low volatility. Only with the invention of liquid beams of volatile liquids compatible with high-vacuum conditions was PES from liquid surfaces under vacuum made feasible. Because of the ubiquity of water interfaces in nature, the liquid water–vacuum interface became a most attractive research topic, particularly over the past 10 years. PES studies of these important aqueous interfaces remained significantly challenging because of the need to develop high-pressure PES methods.

For decades, ESCA or PES (termed XPS, for X-ray photoelectron spectroscopy, in the case of soft X-ray photons) was restricted to conventional laboratory X-ray sources or beamlines in synchrotron facilities. This approach enabled frequency domain measurements, but with poor time resolution. Indirect access to time-resolved processes in the condensed phase was only achieved if line-widths could be analyzed or if processes could be related to a fast clock, that is, reference processes that are fast enough and are also well understood in the condensed phase. Just recently, the emergence of high harmonic light sources, providing short-wavelength radiation in ultrashort light pulses, added the dimension of time to the classical ESCA or XPS technique and opened the door to (soft) X-ray photoelectron spectroscopy with ultrahigh time resolution.

The combination of high harmonic light sources (providing radiation with laserlike beam qualities) and liquid microjet technology recently enabled the first liquid interface PES experiments in the IR/UV-pump and extreme ultraviolet-probe (EUV-probe) configuration. In this Account, we highlight features of the technology and a number of recent applications, including extreme states of matter and the discovery and detection of short-lived transients of the solvated electron in water. Properties of the EUV radiation, such as its controllable polarization and features of the liquid microjet, will enable unique experiments in the near future. PES measures electron binding energies and angular distributions of photoelectrons, which comprise unique information about electron orbitals and their involvement in chemical bonding. One of the future goals is to use this information to trace molecular orbitals, over time, in chemical reactions or biological transformations.

1. Introduction

Most of the interesting processes in chemistry and biology occur in the condensed phase, in particular in liquid water. It is therefore important to probe the chemical and biochemical dynamics of these processes in this environment. The advent of femtosecond laser spectroscopy made it possible to use photons to visualize chemical dynamics on a time scale of molecular and atomic motions.[1] However,

Published on the Web 11/10/2011 www.pubs.acs.org/accounts
10.1021/ar200154w

optical domain spectroscopy cannot provide much information about molecular structure. This goal becomes accessible if traditional techniques such as X-ray and electron diffraction[2] and X-ray absorption spectroscopy[3] are implemented as probes in the above pump–probe scheme. In the past decade, time-resolved X-ray absorption spectroscopy has emerged as a valuable tool for the study of structural dynamics in liquids and has matured to a routine method on the picosecond time scale,[4] while femtosecond time resolution has just been demonstrated.[3,5] Structure information as a function of time is attractive; however, even closer to the chemist's heart may be to monitor the evolution of the electron density in a molecule, as (bio)molecules transform, as a function of time.[6]

Therefore, we want to focus our attention on another exciting experimental route toward the goal of understanding key observables of chemical transformations in liquid systems in detail by measuring electron densities in time as structural changes occur. The observables in these experiments comprise unique information about electron orbitals, binding motifs, and local order and structure.

Recent progress in time-resolved condensed phase photoelectron spectroscopy with extreme UV light in our group[7,8] has been largely driven by the development of new experimental techniques, in particular new ultrafast light sources based upon generation of EUV or XUV-light through the process of high-order harmonic generation (HHG). HHG pushes traditional nonlinear frequency conversion to an extreme, by combining many laser photons together to generate pulsed coherent radiation from the UV to the 1 keV region of the spectrum and ranging from femtosecond to attosecond in duration.[9] Since Faubel and Kisters in Göttingen developed liquid beams in vacuum, also volatile liquids such as water can be investigated with photoelectron spectroscopy.[10,11]

These experimental advances were prerequisite for the new approach. With this strategy, we literally added the dimension of time to liquid (interface) electron spectroscopy for chemical analysis (ESCA)[12] or liquid-phase E(X)UV photoelectron spectroscopy.[7,8,13]

2. A High Harmonics Table-Top Source and Liquid Water Jet in Vacuum: A Successful Marriage

Liquid water jets in vacuum have been developed initially and introduced by Faubel and Kisters at the end of the 1980s,[10,11] and they were optimized in recent years.[14] A liquid jet in vacuum is displayed in Figure 1a. The left picture

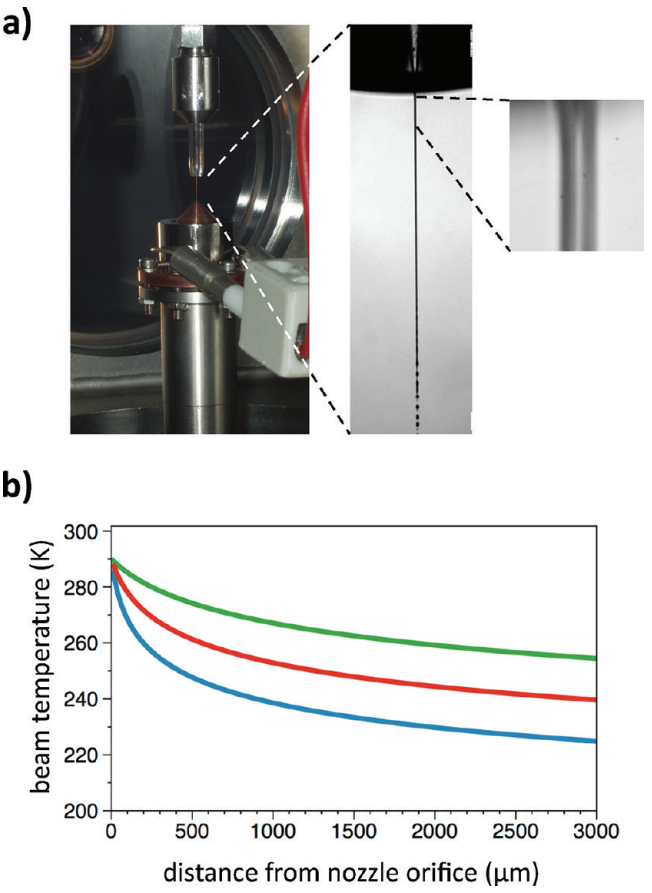

FIGURE 1. (a) Liquid beam (diameter ≈ 15 μm) and nozzle assembly (left). The enlarged section displays the liquid beam's continuous section (middle) and the decay into droplets behind the Rayleigh limit. The enlarged diameter (15 μm) and the beam contraction when exiting the nozzle can be seen on the right-hand side. (b) Effect of evaporative cooling (beam temperature) as a function of distance from the nozzle exit for a 17 μm nozzle at 0.3 mL/min flow and a flow speed of the jet of ≈22 m/s. Color code: green, water; red, ethanol; blue, methanol. Calculated according to ref 15.

in Figure 1a shows the nozzle, the liquid beam in vacuum, and the beam catcher.[14] A high speed image of a beam with a 2–3 mm long continuous beam section that decomposes into droplets (Rayleigh limit) is displayed in the middle picture of Figure 1a, whereas the right-hand picture shows the 15 μm water beam right at the exit of the nozzle where the liquid contraction is visible. The liquid beam is typically driven by a HPLC (constant flow metering) pump at 10–50 bar at flow speed of, typically, 20–50 m/s and up to 120 m/s.[14] The rapidly changing temperature (T_0 = 290 K) of the beam (surface), driven by evaporative cooling, is plotted against the distance from the nozzle exit in Figure 1b for liquid water, ethanol, and methanol.[15] Due to the small jet diameter in comparison to the molecular mean free path of the evaporating water molecules, the microjet liquid surface is a true free

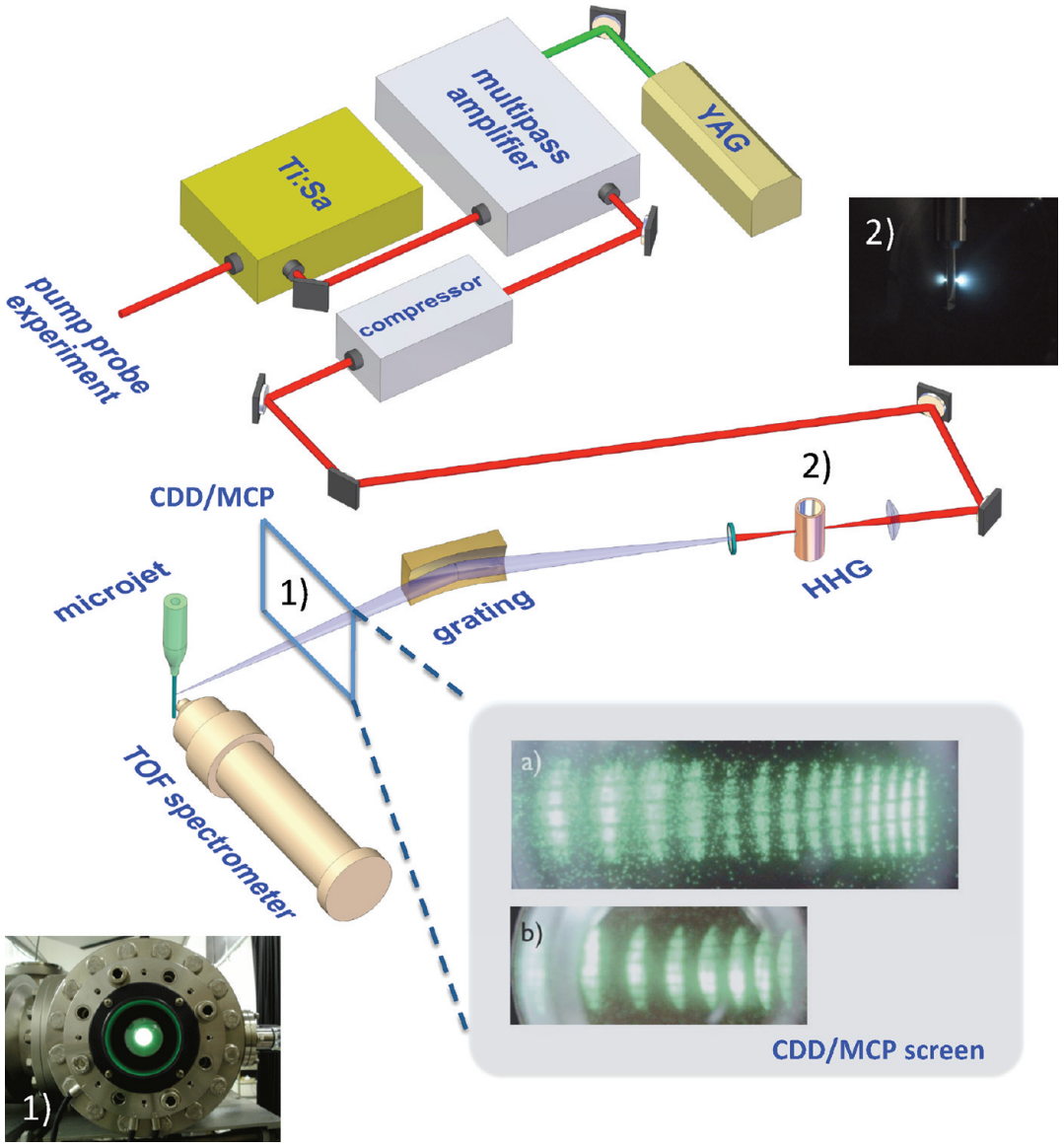

FIGURE 2. Schematic view on the table-top beamline experiment and the components for the photoelectron spectroscopy experiment. Inset: Generation of high harmonics of the fundamental 800 nm radiation in a neon or argon filled capillary. (a) Sequence of high harmonics generated in neon, imaged by an EUV-sensitive CCD camera. The range of photon energies spans 40−70 eV. (b) Sequence of high harmonics generated in argon. The range of photon energies in this case is between 25 and 40 eV.

vacuum surface. Note, there are no gas phase water molecule collisions in the radially diverging gas stream and no collision of outgoing photelectrons with the vapor.

Harmonic generation[9,16] is a nonlinear optical process in which the frequency of laser light is converted into its integer (odd) multiples by focusing intense laser pulses into a nonlinear noble gas medium. The frequency spectrum from the process of high harmonic generation (HHG) is relatively broad and consists typically of a plateau, where the harmonic intensity is nearly constant over many orders of magnitude followed by a sharp cutoff.[16] Many features of HHG can be intuitively and semiquantitatively explained in terms of electron rescattering trajectories, which are described by Corkum's semiclassical three-step model.[17]

The setup used in Göttingen and Leipzig for ultrafast photoelectron spectroscopy near the liquid water microjet surface with UV or IR pump and high harmonic EUV-probe is illustrated schematically in Figure 2. The inset displays high harmonics on a multichannel-plate detector behind the grating for neon (a) and argon (b) as a HHG medium. HHG gas cell, grating, and target (liquid jet) are located in connected vacuum chambers. The different harmonics generated in a laser drilled capillary (closed at the bottom) are dispersed and focused, employing a toroidal grating. The

fundamental is blocked with a thin aluminum filter. The time-resolution of our first generation single grating setup is on the order of a few hundred femtoseconds, depending upon the HHG spot size and the number of illuminated grooves on the EUV-grating,[7,8] which can be optimized further by employing dielectric mirrors or a second grating.[18]

3. Extreme States of Water and Transient Hydrogen Bonding

Liquid water is special, i.e., has many unusual properties when compared with other `simple' organic liquids,[19,20] and bulk water as well as single water molecules are known to play a decisive role in many chemical and biological systems.[19,21] The dynamical network of hydrogen bonded water in chemical and biological systems has been studied with powerful spectroscopic techniques as well as theoretical approaches.[22−24]

The H_2O molecule has a well known electron configuration. $1b_1$, $3a_1$, and $1b_2$ denote the three outer valence molecular orbitals of water, which are depicted schematically together with the molecular diagram of water in Figure 3. Before turning to more complicated time-dependent situations, we will rationalize "static" photoelectron spectra of gas phase and liquid water (with some gas phase water) in the valence orbital energy region. Figure 3b and c shows photoelectron spectra of gas phase water and of liquid water in the form of a thin jet in vacuum, respectively. The latter contains both gas phase and liquid phase signals. Blue shaded areas indicate the positions of liquid signals. For a discussion of line shifts and broadening, see ref 25.

If very short infrared laser pulses are used, which are tuned to a strong OH-stretch vibration absorption of water around 3 μm, it is possible to heat the water at a rate faster than the thermal expansion rate and to prepare extreme states of water.[7,8] These states can have temperatures well above the boiling point, and it has been shown that the water phase may be even heated significantly above the critical temperature (see ref 8 and references therein). As shown in ref 8, the initial temperature after laser induced heating can be estimated via the known starting temperatures (Figure 1b), laser intensities, absorption coefficients, and penetration depths of the IR beam. If water is prepared at these extreme states, it is known that it literally explodes; however, at the extreme conditions; however, at the femtosecond or picosecond time scale, it moves slowly in time and can thus be resolved with ultrafast spectroscopy. In a recent contribution, we reported investigations of the molecular photoemission signature of the evolution of the

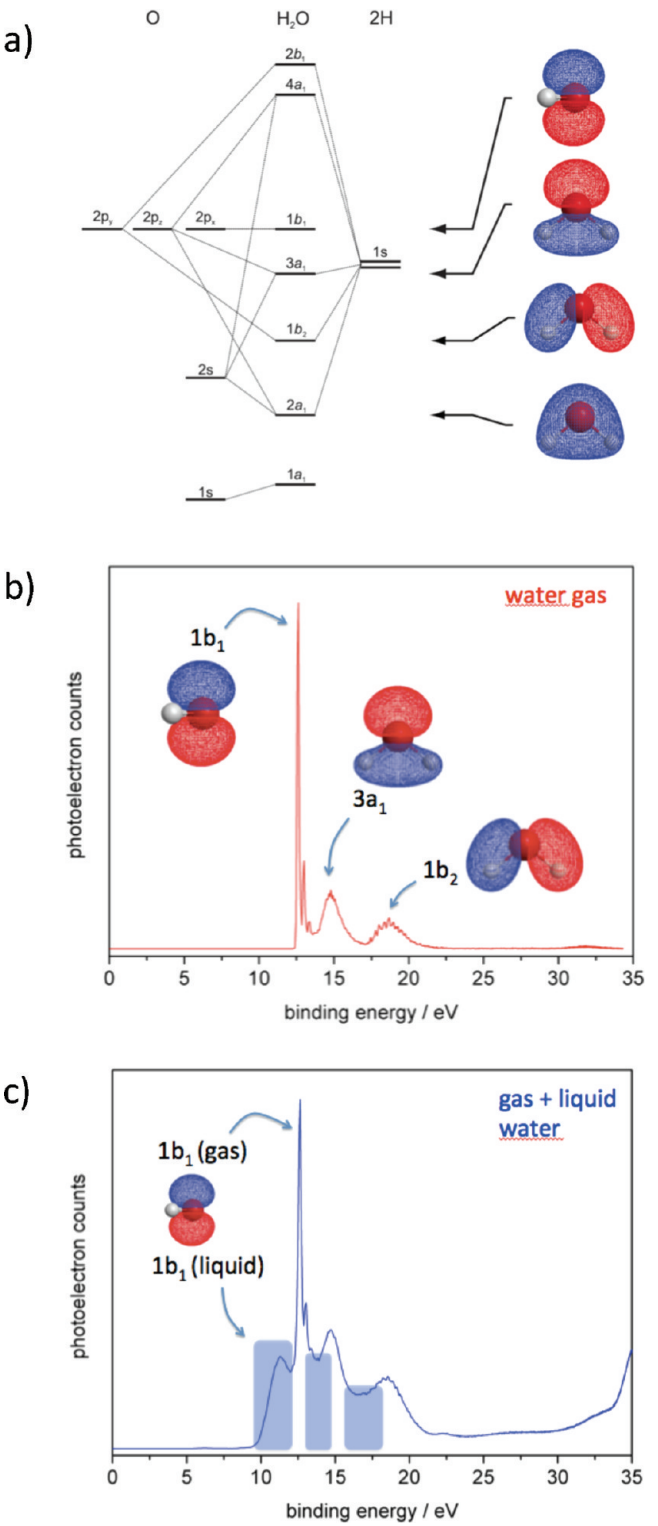

FIGURE 3. (a) Molecular orbital diagram of water and plots of the valence orbitals. (b) Photoelectron spectrum of gas phase water and (c) of the liquid water jet. For a discussion of line shifts and broadening, see ref 25.

phase and the hydrogen-bonding network of superheated water below and above the critical point, as well as its time

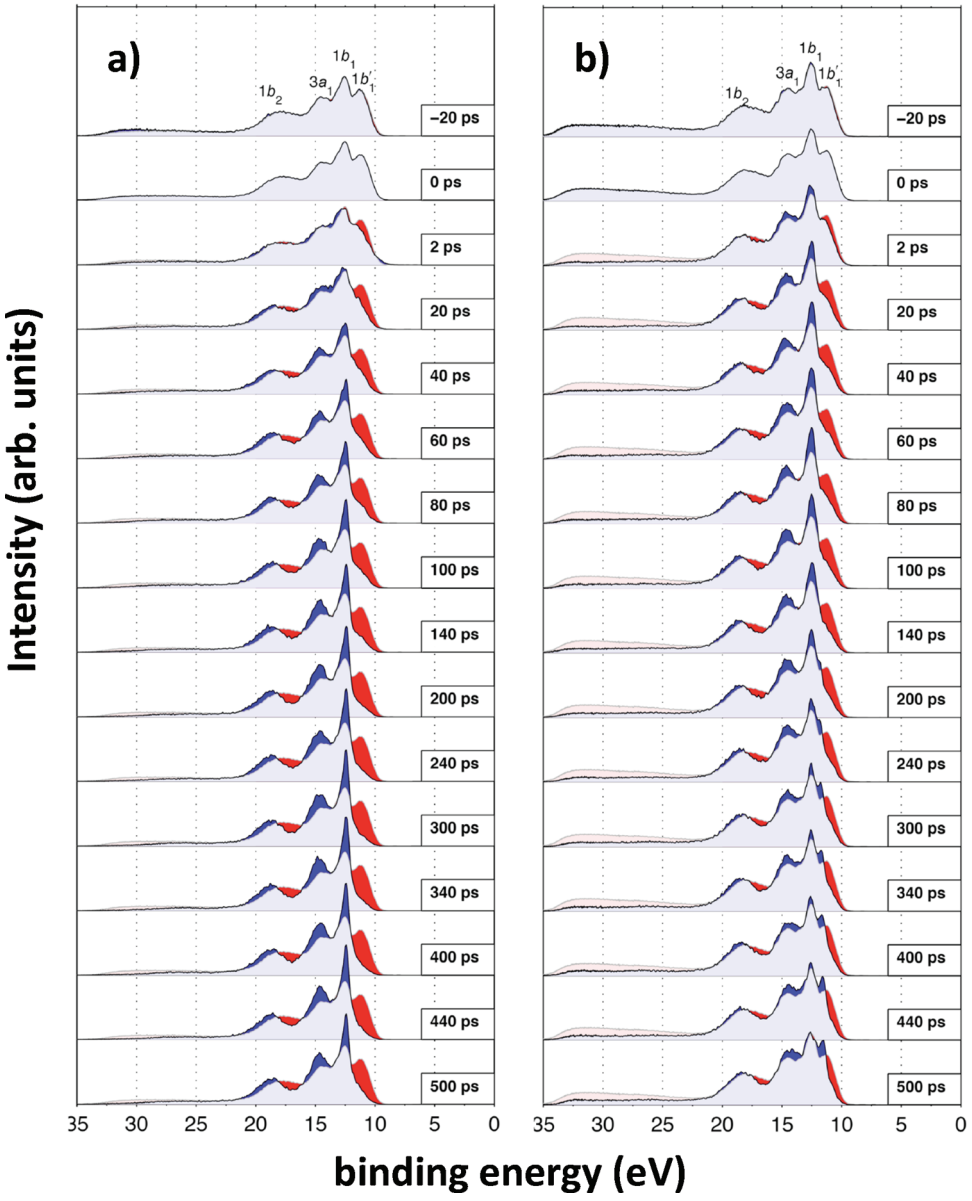

FIGURE 4. Time-resolved photoelectron spectra of liquid (before excitation at neg. delay time) and metastable water ((a) excitation at $\lambda_{IR} = 2650$ nm; (b) $\lambda_{IR} = 2830$ nm). For further details, see the text and ref 8.

scales. Typical results are displayed in Figure 4 for a series of time delays over a wide range from 2 to 500 ps. In the plots, the binding energy (being the difference of the photon energy and the kinetic energy of the photoelectrons measured in the experiment via a time-of-flight electron spectrometer, $E_b = E_{ph} - E_{kin}$, here $E_{ph} = 38.7$ eV) is plotted against the photoelectron emission counts. In a typical valence electron photoemission spectrum of water, in Figure 4, the gas phase emission lines of the $1b_1$, $3a_1$, and $1b_2$ can be assigned easily.[26] In general, the PE signals of the orbitals in the liquid phase are shifted towards lower binding energies. For water, this gas − liquid shift amounts to about 1.9 eV. In addition, the liquid peaks show significant broadening and partial overlap. The shifted $1b'_1$ orbital energy peak is distinctly visible at the lowest binding energies in the liquid phase and can be tracked easily. A transition of water from the liquid phase to the gas phase is accompanied with a decrease in intensity in the furthermost shifted $1b'_1$ emission line (color coded in red) of liquid water. At the same time, an increase in intensity is observed for all gas phase lines ($1b_1$, $3a_1$, and $1b_2$) (color coded in blue in Figure 4). Differently hot phases are correlated with the overall time-dependence of the signals and the dispersion of the liquids, which is observable in the binding energy region between the liquid phase $1b_1$ peak and the gas phase peak. This is typically the range in which $1b_1$ photoemission of clusters has been

observed.[27] In particular, the hotter phase in Figure 4 (right) displays a higher degree of dispersion into smaller clusters. The overall chemical shift of the $1b'_1$ of the intermediate superheated phase toward larger binding energies is noticeable but small. In ref 8, we have shown that quantitative photoelectron emission detection and evaluation through a hot and moving interface is possible and that the photoelectron observation depth extends through a few, outermost, monolayers of water molecules at the interface only.[28] The dynamics of superheated water (and alcohols) at the liquid−vacuum interface has been compared with large-scale molecular dynamics calculations that capture the dynamics of the solvents near their liquid and super heated interface. It is not unexpected that the dynamics of the phase evolution after laser heating is governed by the highly dynamical evolution of the network of hydrogen bonds.[8]

Supercritical water has recently drawn much attention in the field of green chemistry. It is crucial to an understanding of supercritical solvents to know their dynamics and to what extent hydrogen bonds persist in these fluids.

4. Toward Ultrafast Angle-Resolved Liquid Phase E(X)UV Photoelectron Spectroscopy

The direction of photoelectron emission in the gas phase and near interfaces is intrinsically nontrivial and more or less anisotropic in general.[29] The photoelectron angular distribution of a randomly oriented ensemble of molecules from one-photon ionization with linearly polarized light is given by eq 1

$$\frac{d\sigma}{d\Omega} = \frac{\sigma_{tot}}{4\pi}(1 + \beta P_2(\cos\theta)) \quad (1)$$

where θ denotes the angle between the electron velocity and the polarization direction of the ionizing light, and σ_{tot} represents the total cross section. The anisotropy parameter β ranges between -1 and 2 and depends on the symmetry of the initial and final states as well as the electron kinetic energy.[29]

Why is it rewarding to measure this quantity, for example, for water, possibly in time-resolved experiments? It has long been recognized in conventional (i.e., non-time-resolved) photoelectron spectroscopy that the measurement of photoelectron angular distributions provides information complementary to that obtained by photoelectron energy distributions.[29]

The standard picture of liquid water posits that each molecule of H_2O is, on average and approximately, bound to four others in a tetrahedral motif in a three-dimensional network of hydrogen bonds. This picture comes largely from neutron-scattering studies and computer simulations.[20] Recently, this picture was challenged and heavily debated.[20] With ultrafast angle resolved E(X)UV photoelectron spectroscopy, this topic may be addressed by literally shedding new light onto this issue. It is anticipated that the latter technology can provide unique information on the electronic structure and local order as well as hydrogen bonding of water molecules in water and thus time-dependent coordination numbers. Halfway on the road toward this ambitious goal and a first proof-of-principle would be measurements of electron emission anisotropies for liquid samples irradiated with pulsed EUV or soft X-ray radiation.

Although possible in principle at few beamlines at Synchrotron radiation sources, polarization resolved experiments are rare, such that the anisotropy parameters for the molecular valence orbitals of water have only been measured for isolated gas phase water molecules, but not for liquid water. It has instead been assumed that they do not differ significantly from the values in the gas phase.[25] For the investigation of the angular distribution of photoelectron emission, either a velocity map imaging (VMI) detector has to be used or measurements of photoelectrons at different angles θ between the polarization vector of the ionizing radiation and the direction of photoelectron detection must be carried out (see Conspectus graphic). In a table-top HHG experiment, the EUV radiation polarization (and thus θ) can be readily controlled via control of the polarization of the laser fundamental if the spectrometer is fixed in the setup. For the investigation of the angular distribution of emitted photoelectrons, measurements at different emission angles θ are required. For this purpose, we change the polarization vector of the fundamental radiation with a $\lambda/2$ plate before it enters the HHG chamber. Since the polarization properties are conserved in HHG, this is a convenient way to modify θ, that is, the angle between polarization plane and direction of photoelectron detector. The initial polarization plane of the 800 nm fundamental light is parallel to that of the optical table. At p-polarization, the angle θ between the photoelectron detecting direction and the polarization vector of the ionizing radiation is 0°, while $\theta = 90°$ for s-polarization. In addition, there is another relevant angle at $\theta = 54.7°$, also called the *magic angle*, which plays an important role in the characterization of the angular distribution of photoionization. We measured the first "static" photoelectron emission spectra of liquid water for different angles θ (Figure 5).

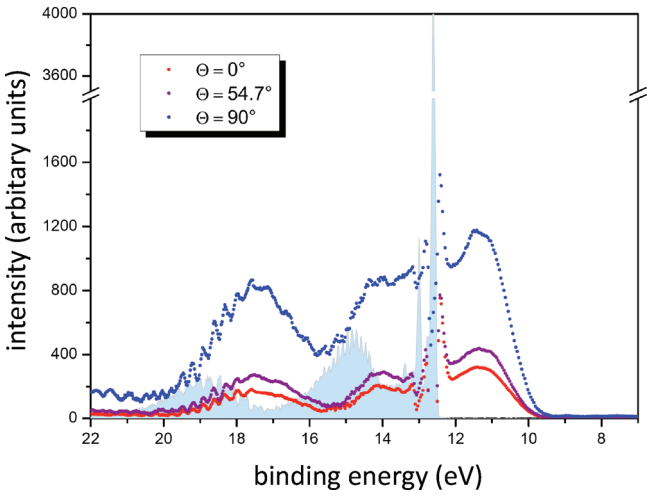

FIGURE 5. Liquid beam photoelectron spectra at different angles. The light blue spectrum is the spectrum of water in the gas phase measured with p-polarized EUV light.

In the PES traces, the electron count rate (denoted as "intensity") is plotted versus the energy. The binding energy shown on the abscissa of the spectrum, $E_b = h\nu - E_{kin}$, is obtained as the difference of the photon energy and the photoelectron kinetic energy measured in the experiment via a time-of-flight spectrometer. The spectra are normalized with respect to the $1b_1$ gas phase photoelectron emission peak. The pure gas phase spectrum (blue) has been measured with a p-polarization of the EUV beam. These spectra can be translated into usual anisotropy diagrams for single orbitals (not shown here).[7] For a HHG energy of 38.7 eV, the anisotropy parameters β and σ (for a definition see eq 1) for the different orbitals have been determined to be $1b_1$(β = 0.8,σ=1), $3a_1$ (β=0.7,σ=0.88), and $1b_2$ (β=0.6,σ=0.94) for liquid water and $1b_1$(β=1.4,σ=1), $3a_1$ (β=1.1,σ=0.88), and $1b_2$ (β = 0.7,σ = 0.94) for gas phase water. The measurements are most consistent with the reasonable assumption that the σ-values are not changed significantly in the liquid phase in comparison to the gas phase. The isolated gas phase molecular anisotropies are close to those measured by Banna et al.[30] some time ago. What is important here, and here the value of the present setup is obvious, is the observation that the β-values of liquid and gas phase water are significantly different, while the σ-values appear to be very similar. Tentative first interpretations for these remarkable gas–liquid changes of electron emission anisotropy factors are starting from the observation that the orbitals participating in hydrogen bonds are most dramatically affected. Along the ideas sketched above, an anisotropy measurement may thus provide a highly sensitive probe for the extent to which a water molecule is actually networked in the two available bond donor and two bond acceptor sites in the liquid environment.

5. The Hydrated Electron: Investigation of Two Binding Motifs

In a simple picture, a completely hydrated electron $e^-_{(aq)}$[31] can be viewed as being "located" in a highly dynamical nonspherical cavity formed on average by about six water molecules.[32] The vertical binding energy (VBE) would correspond to the energy which is required to completely remove the electron from this cavity without changing the initial geometry of the system.[33] A measurement of the vertical binding energy is a crucial step toward an understanding of many electron transfer and attachment processes (see ref 34 and references therein).

In earlier studies, binding energies of hydrated electrons were roughly estimated via extrapolation of the binding energies of hydrated electrons in large anionic water clusters.[35] Just recently, Siefermann et al. for the first time directly measured the VBEs of $e^-_{(aq)}$ (VBE = 3.3 ± 0.1 eV) and of electrons solvated/hydrated at the water surface $e^-_{(surface)}$ (VBE = 1.6 ± 0.1 eV) using the experimental setup displayed in Figure 2.[6] Solvated electrons were generated from precursors by a short pump pulse of 267 nm light[36] and photoelectron spectra were recorded with a time-delayed 38.7 eV (32 nm) high harmonic probe pulse. In order to access the properties of $e^-_{(surface)}$, pure water is ionized via the two-photon absorption of 267 nm light.[36] The assignment of the transient corresponding to a surface-bound electron is consistent with the very low probing depth of EUV photoelectron spectroscopy.[25,37] This means, the detection efficiency is highest for photoelectrons originating from the surface, and declines dramatically with every layer of water molecules[37] such that $e^-_{(surface)}$ is detected with a higher probability compared to $e^-_{(bulk)}$. In order to access the VBE of $e^-_{(aq)}$ with our experimental setup, it is required to significantly increase the concentration of $e^-_{(aq)}$ and at the same time suppress the formation of $e^-_{(surface)}$. This is realized by photoionization of $[Fe(CN)_6]^{4-}$ complexes in aqueous solution. These complexes are repelled from the water surface,[36,8] and photoionization mainly creates $e^-_{(aq)}$. Suppressing two-photon processes by lowering the 267 nm pump pulse intensity largely inhibits the formation of $e^-_{(surface)}$ and allows for recording the spectrum of the fully hydrated electron $e^-_{(aq)}$. Figure 6 presents the photoelectron spectra of $e^-_{(aq)}$ (a) and $e^-_{(surface)}$(b). For different pump–probe time delays between 7 and 100 ps, no significant changes in the photoelectron spectrum of $e^-_{(surface)}$ were

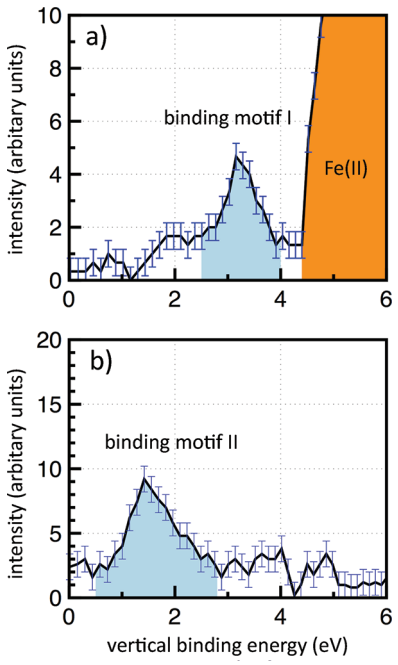

FIGURE 6. Photoelectron spectrum and binding energy of the fully hydrated electron (a) and the surface hydrated electron (b) near the liquid water interface.[6]

observed, which demonstrates that the lifetime of $e^-_{(surface)}$ is unexpectedly long. Follow-up experiments by a number of other groups employing UV light (267−213 nm) to probe the binding energy of the hydrated electron yielded values of 3.27 eV (Tang et al.[38]), 3.6 eV (Shreve et al.[39]), and 3.4 eV (Lübcke et al.[40]), which are close to the value initially reported in ref 6. The characterization of different species and binding motifs of the hydrated electron is showing us that the picture of a single equilibrated hydrated electron species in liquid water may be an oversimplification. While surface-bound hydrated electrons with low electron binding energies have frequently been observed in cold anionic water clusters, this is the first report of a surface-type electron in liquid water. The temperature of the liquid water beam for these experiments was estimated to be about 273−278 K. We have discussed recently that detection of this species may be related to the probe wavelength[41] and/or the different and special precursors.[42] In ref 42, we also discuss structural and energetic properties of this species as well as new insights into dissociative electron attachment of $e^-_{(aq)}$ and $e^-_{(surface)}$ to molecules in aqueous environments. Interestingly, recent theoretical work suggests that there seems to be something like a correlation between the size (degree of delocalization) of the excess electron and its binding energy; that is, the larger (diffuser and extended) the electron density distribution, the smaller is the binding energy of the hydrated electron.[43,44] Why is the surface electron metastable? It should relax quickly and penetrate into the bulk.[43,24] In ref 6, this was tentatively explained by a dynamic barrier preventing the surface hydrated electron from penetrating into the liquid phase and form the completely hydrated state of the electron, which is definitely the more stable state. We have argued recently[42] that a delocalized Rydberg state of water may be viewed to be such a state and that this delocalization may prevent the surface electron from further penetrating into the bulk phase. Rydberg states in condensed matter have been studied before.[45,46] The existence of such a species may depend crucially on the preparation[41] and the precursor[42] implying that the two transients may be two different species that interconvert slowly. A delocalized state may also arise from two-photon dissociation of water and subsequent reaction of H with H_2O at the surface to form H_3O, which can also be stabilized at the surface by a H_3O^+ at the interface and the electron density above, which is difficult to squeeze into the liquid phase without breaking several hydrogen bonds. Such a "state" corresponds to a different chemical species. Again, different chemical species would circumvent the need for a barrier separating the two systems. One of the main arguments in favor of a transient surface electron (that may not reside above the surface literally but which may be embedded in the liquid in a half cavity, which is suggested by the measured binding energy) is the extrapolation of cluster data to the bulk. We are aware of the fact that bulk water and cluster are in a different state (i.e., solid or amorphous and liquid) and that there are more cluster isomers that do not all necessarily extrapolate toward two limiting cases (3.2 and 1.6 eV).[47] Nevertheless, we believe and propose that the correlation of the extrapolation of certain main cluster isomer families toward the liquid is not accidental. This would indeed imply that the delocalization and the position of the electron are correlated and that they are energetically more important than their state of aggregation. Compact states at the surface do not seem to be stable.[44,47]

6. Watching Concerted Electron Motion in a near Liquid Water Surface Plasma

A number of methods to investigate the parameters of laser-induced plasmas[48] have been reported (see also ref 7 and references therein). A plasma near a water interface constitutes a special case of coherent electron motion that can in principle be observed with ultrafast photoelectron spectroscopy. Using near IR femtosecond pulses, a surface plasma can be generated through multiphoton absorption and

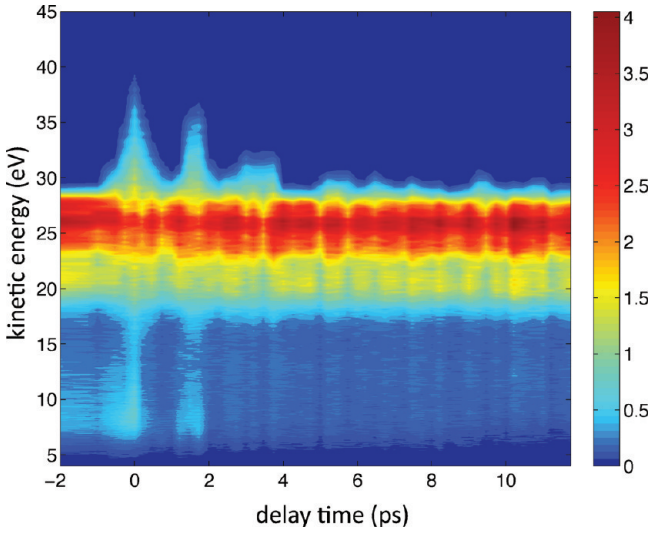

FIGURE 7. Kinetic energies of photoelectrons as a function of time on top of the raw water photoelectron spectrum (vertical cut) in the case of an oscillating near liquid water surface plasma.

ionization. If it is formed near a liquid beam in vacuum (that in turn explodes), the plasma first oscillated at the plasma frequency and then decays due to the overall decay of the hot water filament. High harmonics radiation can be employed to induce electron emission from the valence bands of dense water at the interface and gas phase water, which should be sensitive to the local plasma environment and transient electron binding/kinetic energies. In ref 7, we reported first experimental studies on the laser-plasma dynamics, that is, the oscillation and decay of a plasma near a liquid water jet, at well characterized parameters. IR pulses with a peak intensity of well above 10^{12} W/cm^2 are employed to induce the surface plasma. The 25th harmonic of 800 nm radiation at 38.7 eV photon energy was chosen for the probe monitoring photoelectron emission from the valence band region of water. In the immediate vicinity of a water jet in high vacuum, the evaporation gas stream produces a vapor density of several 10^{16} H_2O molecules/cm^{-3}, or several mbar, as discussed previously.[15] In Figure 7, showing color coded-3D photoelectron (kinetic) energy spectra as a function of increasing delay time, occur oscillations for periodically changing binding energies. These are recurrent, apparently, as a function of time after the ignition of an IR-laser induced plasma near the liquid microjet interface.[7] The characteristics of the oscillating "binding energies" appearing in the color-coding of the photoelectron kinetic energy spectra suggest that the electrons originate from water molecules in majority. In addition, a significant fraction of electrons shows oscillating values of lower binding energies and high kinetic energies up to the primary photon energy, suggesting that these are free electrons in a laser produced plasma or quasi-free electrons in highly excited weakly bound (Rydberg) states of water. They are not or hardly bound anymore to the water in the gas phase but both are part of an ensemble of ionized cations and electrons oscillating coherently in time. At early times, the IR pump pulse initiates plasma formation near the liquid beam interface (a number of 22 photons at 2650 nm would be necessary to result in an ionization energy of 10 eV). It is well-known that the plasma frequency ω_P in eq 2

$$\omega_P = \left(e^2 n_0/\varepsilon m_0\right)^{1/2} \quad (2)$$

is proportional to the square root of electron density n_0. The additional constants are the electron mass and elementary charge.[16] Evaluating the observed period of oscillation of 1.5 ps, equivalent to 0.67 THz, we obtained a free electron density of 5.6×10^{15} cm^{-3}, in reasonable agreement with the above estimated vapor density in the local cloud near the vacuum surface of liquid water.[7] This is a quite low level of electron density. It is worth noting that with this setup we have realized a pulsed ultrafast THz oscillator that should emit pulsed picosecond THz radiation (not measured in ref 7). The time scale for the decay of the plasma within a few picoseconds, only, is attributed to plasma dispersion into the neutral gas and to the transport of hot water molecules in the expanding (exploding) beam interface, as has been assessed from molecular dynamics simulations.[8]

The plasma visualization study provides another fine example for the power of the ultrafast pump-EUV-photoelectron emission probe spectroscopy, yielding information that is hardly accessible by other methods.

7. Conclusions and Outlook

In summary, the highlighted applications in this Account so far demonstrate the power of the novel approach. One of the main characteristics is the surface sensitivity and its wavelength dependence in the extreme UV. Wavelength tuning can therefore be used for *depth profiling* and species detection in ultrafast experiments. Time-resolution can be increased nowadays to a few femtoseconds, and efforts are underway to produce stable single attosecond pulses in this spectral range.[9] The quest for higher harmonics and shorter pulses bringing us very short wavelengths will enable us to perform real ultrafast ESCA experiments in the water window at around 3−4 nm soon. The high harmonics probe should

also not be limited to "bright states". It is an in situ, local, and site-specific probe of femtosecond and even attosecond electron dynamics in molecules surrounded by a solvent or dense environment. Finally, the compact light source is a very valuable tool/setup to prestudy systems and optimize conditions for experiments at synchrotron beamlimes such as the free electron laser, LCLS in Stanford, FLASH in Hamburg, and the future European XFEL, which will have admittedly superior performance but very limited beam time.

Financial support from the SPP1134, the SFB 755, and the Graduate School 782 of the DFG is gratefully achnowledged.

BIOGRAPHICAL INFORMATION

M. Faubel studied physics at the University of Mainz and Göttingen and obtained a Ph.D. at the University of Göttingen in 1976. Since 1973, he has been a research staff scientist at the MPI für Strömungsforschung.

K. R. Siefermann received the diploma degree in chemistry in 2007 from the Karlsruhe Institute of Technology (KIT) and her Ph.D. from the University of Göttingen working with B. Abel. She is currently a postdoc at the Lawrence Berkeley National Laboratory.

Y. Liu studied Chemistry in Göttingen and obtained her Ph.D. in 2010 at the University of Göttingen working in the group of B. Abel.

B. Abel studied chemistry at the University Göttingen and obtained his Ph.D. in 1990. After 2 years at the MIT in Cambridge, MA, he was associate professor in physical chemistry in Göttingen. Since 2008, he is full professor at the University of Leipzig.

FOOTNOTES

*To whom correspondence should be addressed. E-mail: bernd.abel@uni-leipzig.de.

REFERENCES

1 Zewail, A. H. Femtochemistry: Atomic-Scale Dynamics of the Chemical Bond. *J. Phys. Chem. A* **2000**, *104*, 5660–5694.

2 Zewail, A. H. 4D Ultrafast Electron Diffraction, Crystallography, and Microscopy. *Annu. Rev. Phys. Chem.* **2006**, *57*, 65–103.

3 Bressler, C.; Chergui, M. Molecular Structural Dynamics Probed by Ultrafast X-Ray Absorption Spectroscopy. *Annu. Rev. Phys. Chem.* **2010**, *61*, 263–282.

4 Bressler, C.; Chergui, M. Ultrafast X-ray Absorption Spectroscopy. *Chem. Rev.* **2004**, *104*, 1791–1812.

5 Bressler, C.; Milne, C.; Pham, V.-T.; ElNahhas, A.; van der Veen, R. M.; Gawelda, W.; Johnson, S.; Beaud, P.; Grolimund, D.; Kaiser, M.; Borca, C. N.; Ingold, G.; Abela, R.; Chergui, M. Femtosecond XANES Study of the Light-Induced Spin Crossover Dynamics in an Iron(II) Complex. *Science* **2009**, *323*, 489–492.

6 Siefermann, K. R.; Liu, Y.; Lugovoy, E.; Link, O.; Faubel, M.; Buck, U.; Winter, B.; Abel, B. Binding energies, lifetimes and implications of bulk and interface solvated electrons in water. *Nat. Chem.* **2010**, *2* (4), 274.

7 Link, O.; Lugovoy, E.; Siefermann, K.; Liu, Y.; Faubel, M.; Abel, B. Ultrafast electronic spectroscopy for chemical analysis near liquid water interfaces: concepts and applications. *Appl. Phys. A: Mater. Sci. Process.* **2009**, *96* (1), 117.

8 Link, O.; Vohringer-Martinez, E.; Lugovoj, E.; Liu, Y. X.; Siefermann, K.; Faubel, M.; Grubmuller, H.; Gerber, R. B.; Miller, Y.; Abel, B. Ultrafast phase transitions in metastable water near liquid interfaces. *Faraday Discuss.* **2009**, *141*, 67–79.

9 Krausz, F.; Ivanov, M. Attosecond physics. *Rev. Mod. Phys.* **2009**, *81* (1), 163.

10 Faubel, M. *Photoionization and Photodetachment*; Ng, C. Y., Ed.; World Scientific: 2000.

11 Faubel, M.; Kisters, T. Non-equilibrium molecular evaporation of carboxylic acid dimers. *Nature* **1989**, *339* (6225), 527.

12 Siegbahn, K.; Svenson, H.; Lundholm, M. J. A new method for ESCA studies of liquid-phase samples. *J. Electron Spectrosc.* **1981**, *24*, 205.

13 Drescher, M. Time-resolved ESCA: a novel probe for chemical analysis. *Z. Phys. Chem.* **2004**, *218*, 1147–1168.

14 Charvat, A.; Lugovoj, E.; Faubel, M.; Abel, B. New design for a time-of-flight mass spectrometer, RSI. *Rev. Sci. Instrum.* **2004**, *75*, 1209–1218.

15 Faubel, M.; Schlemmer, S.; Toennies, J. P. A molecular beam study of the evaporation of water from a liquid jet. *Z. Phys. D* **1988**, *10*, 269–277.

16 Attwood, D. *Soft X-rays and extreme ultraviolet radiation:Principles and applications*; Cambridge University Press: Cambridge, 1999.

17 Corkum, P. B. Plasma Perspective on Strong-Field Multiphoton Ionization. *Phys. Rev. Lett.* **1993**, *71* (13), 1994.

18 Nugent-Glandorf, L.; Scheer, M.; Samuels, D. A.; Mulhisen, A. M.; Grant, E. R.; Yang, X.; Bierbaum, V. M.; Leone, S. R. Ultrafast Time-Resolved Soft X-Ray Photoelectron Spectroscopy of Dissociating Br2. *Phys. Rev. Lett.* **2001**, *87*, 193002.

19 Ball, P. Water: Water — an enduring mystery. *Nature* **2008**, *452*, 291.

20 Wernet, P.; Nordlund, D.; Bergmann, U.; Cavalleri, M.; Odelius, M.; Ogasawara, H.; Nyslund, L. A.; Hirsch, T. K.; Ojamse, L.; Glatzel, P.; Pettersson, L. G.; Nilsson, A. The structure of the first coordination shell in liquid water. *Science* **2004**, *304* (5673), 995–999.

21 Vohringer-Martinez, E.; Hansmann, B.; Hernandez, H.; Francisco, J. S.; Troe, J.; Abel, B. Water catalysis of a radical-molecule gas-phase reaction. *Science* **2007**, *315*, 497–501.

22 Cowan, M. L.; Bruner, B. D.; Huse, N.; Dwyer, J. R.; Chugh, B.; Nibbering, E. T.; Elsaesser, T.; Miller, R. J. Ultrafast memory loss and energy redistribution in the hydrogen bond network of liquid H2O. *Nature* **2005**, *434* (7030), 199–202.

23 Fecko, C. J.; Eaves, J. D.; Loparo, J. J.; Tokmakoff, A.; Geissler, P. L. Ultrafast hydrogen-bond dynamics in the infrared spectroscopy of water. *Science* **2003**, *301* (5640), 1698–1702.

24 Madarasz, A.; Rossky, P. J.; Turi, L. Exess electron relaxation dynamics at water/air interfaces. *J. Chem. Phys.* **2007**, *126*, 234707.

25 Winter, B.; Faubel, M. Photoemission from Liquid Aqueous Solutions. *Chem. Rev.* **2006**, *106*, 1176.

26 Winter, B.; Weber, R.; Widdra, W.; Dittmar, M.; Faubel, M.; Hertel, I. V. Full Valence Band Photoemission from Liquid Water Using EUV Synchrotron Radiation. *J. Phys. Chem. A* **2004**, *108* (14), 2625.

27 Belau, L.; Wheeler, S. E.; Ticknor, B. W.; Ahmed, M.; Leone, S. R.; Allen, W. D.; Schaefer, H. F.; Duncan, M. A. Ionization thresholds of small carbon clusters: Tunable VUV experiments and theory. *J. Am. Chem. Soc.* **2007**, *129* (33), 10229–10243.

28 Itikawa, Y.; Mason, N. Cross sections for electron collisions with water molecules. *J. Phys. Chem. Ref. Data* **2005**, *34*, 1–22.

29 Neumark, D. M. Time-Resolved Photoelectron Spectroscopy of Molecules and Clusters. *Annu. Rev. Phys. Chem.* **2001**, *52*, 255–277.

30 Banna, M. S.; McQuaide, B. H.; Malutzki, R.; Schmidt, V. The photoelectron spectrum of water in the 30 to 140 eV photon energy range. *J. Chem. Phys.* **1986**, *84*, 4739–4744.

31 Boag, J. W.; Hart, E. J. Absorption Spectra in Irradiated Water and Some Solutions - Absorption Spectra of Hydrated Electron. *Nature* **1963**, *197* (486), 45.

32 Kevan, L. Solvated Electron Structure in Glassy Matrices. *Acc. Chem. Res.* **1981**, *14*, 138.

33 Jordan, K. D. A Fresh Look at Electron Hydration. *Science* **2004**, *306*, 618.

34 Sanche, L. Beyond radical thinking. *Nature* **2009**, *461*, 358–359.

35 Neumark, D. Spectroscopy and dynamics of excess electrons in clusters. *Mol. Phys.* **2008**, *106*, 2183.

36 Chen, X.; Bradforth, S. E. The ultrafast dynamics of photodetachment. *Annu. Rev. Phys. Chem.* **2008**, *59*, 203.

37 Ottosson, N.; Faubel, M.; Bradforth, S. E.; Jungwirth, P.; Winter, B. Photoelectron spectroscopy of liquid water and aqueous solution: Electron effective attenuation lengths and emission-angle anisotropy. *J. Electron Spectrosc. Relat. Phenom.* **2010**, *177* (2−3), 60.

38 Tang, Y.; Shen, H.; Sekiguchi, K.; Kurahashi, N.; Mizuno, T.; Suzuki, Y.-I.; Suzuki, T. Direct measurement of vertical binding energy of a hydrated electron. *Phys. Chem. Chem. Phys.* **2010**, *12*, 3653.

39 Shreve, A. T.; Yen, T. A.; Neumark, D. M. Photoelectron spectroscopy of hydrated electrons. *Chem. Phys. Lett.* **2010**, *493*, 216.

40 Lübcke, A.; Buchner, F.; Heine, N.; Hertel, I.; Schultz, T. Time-resolved photoelectron spectroscopy of solvated electrons in aqueous Nal solution. *Phys. Chem. Chem. Phys.* **2010**, *12*, 14692.

41 Shoji, M.; Kaniwa, K.; Hiranuma, Y.; Mafune, F. Solvation Structures of Iodide on and below a Surface of Aqueous Solution Studied by Photodetachment Spectroscopy. *J. Phys. Chem. A* **2011**, *115*, 2148.

42 Siefermann, K. R.; Abel, B. The Hydrated Electron: A Seemingly Familiar Chemical and Biological Transient. *Angew. Chem., Int. Ed.* **2011**, *50*, 5264–5272.

43 Frigato, T.; VandeVondele, J.; Schmidt, B.; Schütte, C.; Jungwirth, P. Ab Initio Molecular Dynamics Simulation of a Medium-Sized Water Cluster Anion: From an Interior to a Surface-Located Excess Electron via a Delocalized State. *J. Phys. Chem. A* **2008**, *112*, 6125.

44 Barnett, R. N.; Gininger, R.; Chesnowsky, O.; Landmann, U. Dielectron Attachment and Hydrogen Evolution Reaction in Water Clusters. *J. Phys. Chem. A* **2011**, *115*, 7378.

45 von Haeften, K.; Laarmann, T.; Wabnitz, H.; Möller, T. The electronically excited states of helium clusters: An unusual example for the presence of Rydberg states in condensed matter. *J. Phys. B* **2005**, *38*, 373.

46 Portella-Obertli, M.-T.; Jeannin, C.; Chergui, M. Ultrafast dynamics of Rhydberg states in the condensed phase. *Chem. Phys. Lett.* **1996**, *259*, 475.

47 Ma, L.; Majer, K.; Chirot, F.; von Issendorff, B. Low temperature photoelectron spectra of water cluster anions. *J. Chem. Phys.* **2009**, *131* (14), 144303.

48 Dobosz, S.; Doumy, G.; Stabile, H.; D'Oliveira, P.; Monot, P.; Reau, F.; Höller, S.; Martin, P. Probing hot and dense laser-induced plasmas with ultrafast XUV pulses. *Phys. Rev. Lett.* **2005**, *95* (2), 025001.